

NT

NASA  
Technical Memorandum 81625

AVRADCOM  
Technical Report 81-C-3

# Design of Spur Gears for Improved Efficiency

(NASA-TM-81625) DESIGN OF SPUR GEARS FOR  
IMPROVED EFFICIENCY (NASA) 17 p  
HC A02/MF A01

N81-17436

CSCL 131

Unclas  
G3/37 41389

Neil E. Anderson  
Propulsion Laboratory  
AVRADCOM Research and Technology Laboratories  
*Lewis Research Center*

and

Stuart H. Loewenthal  
*Lewis Research Center*  
*Cleveland, Ohio*



Prepared for the  
ASME Western Design Engineering Conference  
Anaheim, California, December 9-11, 1980  
and the ASME Design Engineering Conference  
Chicago, Illinois, April 28-30, 1981



## DESIGN OF SPUR GEARS FOR IMPROVED EFFICIENCY

by Neil E. Anderson\*  
Propulsion Laboratory  
AVRADCOM Research and Technology Laboratories  
Lewis Research Center  
Cleveland, Ohio

and

Stuart H. Loewenthal\*  
Lewis Research Center  
Cleveland, Ohio

### INTRODUCTION

Generally the geometry of a gear set is designed for the best compromise of tooth strength, surface durability and cost. After checking scoring criteria a power loss calculation might also be made, possibly as an afterthought. The gear designer is either not aware or does not fully appreciate that certain gear geometric variables can significantly affect the power loss of the gearset being designed. For example, as shown in an earlier work by the authors [1] a change in diametral pitch of 32 to 4 can decrease peak efficiency from 99.8 to 99.4 percent for a 10 cm (4.0 in.) pinion gearset under certain operating conditions. Although at first glance this appears to be of little significance, such a change represents at 200 percent change in power loss!

A study of the effects of a wide range of gear geometric and operating conditions on gear efficiency has not been available prior to the work of [1]. Although many methods have been proposed to estimate gear efficiency [2-6] they are not refined to the point that the effects of each gear geometric variable and operating condition on the overall gearset efficiency can be evaluated. Furthermore, most of these methods seriously underestimate gear system power losses at less than full load since they neglect speed dependent losses, that is, the losses associated with forming an elasto-hydrodynamic film (rolling traction), gear windage and support bearing losses. These speed-dependent losses contribute significantly to the cumulative power consumption of many machines which operate at less than full power levels much of the time.

Perhaps the most complete spur gear efficiency analysis presented prior to the present method is re-

ported in [6]. In [6] instantaneous values of sliding and rolling power loss were integrated over the path of contact and averaged. The effects of gear geometry were incorporated into this analysis.

The method of [7] included not only sliding and rolling traction gear losses but also considered the effects of windage and rolling element bearing losses as well.

In order to determine gear mesh losses with the method of [7] it is necessary either to perform a numerical integration or to calculate and sum the power loss at three points along the path of contact. It therefore became the objective of the present study to (1) develop for design purposes a power loss expression that need be evaluated at only one point along the path of contact; (2) to compare this expression with the numerically evaluated expression of [7]; (3) to use this analysis to illustrate which gear geometric and operating variables lead to the highest efficiencies, and (4) illustrate the use of the method with a design example.

### SYMBOLS

CR	contact ratio
$C_s$	support-bearing basic static capacity, N (lbf)
$C_1$	constant used in Eq. (1): $2 \times 10^{-3}$ (SI units); $3.03 \times 10^{-4}$ (English units)
$C_2$	constant used in Eq. (2): $9 \times 10^4$ (SI units); 1.970 (English units)
$C_3$	constant used in Eqs. (3,4): $2.82 \times 10^{-7}$ (SI units); $4.05 \times 10^{-13}$ (English units)
$C_4$	constant used in Eqs. (3,4): 0.019 (SI units); $2.86 \times 10^9$ (English units)
$C_5$	constant used in Eq. (5): $2.10 \times 10^{-4}$ (SI units); $3.18 \times 10^{-10}$ (English units)

\*Member ASME.

$C_6$	constant used in Eq. (7): $9.79 \times 10^{-2}$ (SI units); $2.91 \times 10^{-2}$ (English units)
$C_7$	constant used in Eq. (7): 24.1 (SI units); $3.49 \times 10^{-3}$ (English units)
$C_8$	constant used in Eq. (9): 0.013 (SI units); 0.5 (English units)
$C_9$	constant used in Eq. (13): 29.66 (SI units); 45.94 (English units)
$C_{10}$	constant used in Eq. (15): $2.051 \times 10^{-7}$ (SI units); $4.34 \times 10^{-3}$ (English units)
$C_{11}$	constant used in Eq. (16): 39.37 (SI units); 1.0 (English units)
$C_{12}$	constant used in Eq. (8): $1.45 \times 10^{-4}$ (SI units); 1.0 (English units)
D	pitch circle diameter, m (in.)
$D_m$	bearing pitch diameter, m (in.)
$F_{ST}$	static equivalent bearing load, N (lbf)
$f$	face width of tooth, m (in.)
$f_0$	ball-bearing lubrication factor
$f$	coefficient of friction
$\bar{h}$	isothermal central film thickness, m (in.)
K	gear capacity factor
$L_T$	length of path of contact, m (in.)
M	bearing friction torque, N-m (in-lbf)
$M_L$	load-dependent part of bearing friction torque, N-m (in-lbf)
$M_V$	viscous part of bearing friction torque, N-m (in-lbf)
$m_g$	gear ratio, $N_g/N_p$
N	number of gear teeth
$\eta$	efficiency, percent
n	rotational speed, rpm
P	power loss
$P_{BRG}$	total power loss due to rolling-element support bearings, kW (hp)
$\bar{P}_R$	power loss due to rolling traction, kW (hp)
$\bar{P}_S$	power loss due to tooth sliding, kW (hp)
$P_W$	power loss due to windage, kW (hp)
$\rho$	diametral pitch
R	pitch circle radius or radius in general, m (in.)
$R_{eq}$	equivalent rolling radius, m (in.)

T	pinion torque, N-m (in-lbf)
$\bar{V}_S$	average sliding velocity, $V_g - V_p$ , m/sec (in/sec)
$\bar{V}_T$	average rolling velocity, $V_g + V_p$ , m/sec (in/sec)
$\bar{W}$	gear contact normal load, N (lbf)
w	tangential gear driving load, N (lbf)
$\theta$	gear tooth pressure angle, deg
$\mu_n$	lubricant absolute viscosity, $10^{-3}$ N sec/m <sup>2</sup> (cP) (lbf sec/in <sup>2</sup> )
$\nu$	lubricant kinematic viscosity, $10^{-2}$ cm <sup>2</sup> /sec (cS) (ft <sup>2</sup> /sec)

#### Subscripts:

g	gear
IN	input
p	pinion
R	rolling
S	sliding
TOT	total
0	ambient conditions

#### GEAR POWER LOSS ANALYSIS

The method presented here, following that of [7], considers four major sources of gear system power loss: sliding, rolling, windage and support bearing losses. It is applicable to spur gears of standard tooth proportions in which the gears are jet or splash lubricated. No accounting has been made for churning losses of gears running submerged in oil. The analysis considers sliding losses which are the result of friction forces developed as teeth slide across one another. Rolling losses are generated in the formation of an elastohydrodynamic (EHD) film, that is, as oil is squeezed between gear teeth and subsequently pressurized. In addition to gear sliding and rolling losses an expression was developed to account for gear windage based on disc drag data presented in [8,9]. Support ball bearing losses were included using a well-known method reported in [10].

In [7] the mesh losses were calculated by numerically integrating the sliding and rolling losses over the path of contact. In this analysis the average power losses across the path of contact are calculated algebraically from the average sliding and rolling velocity of the mesh. A simple tooth loading diagram shown in Fig. 1 was assumed. The effect of tooth load sharing was included. The frictional sliding loss was based on disc machine data generated by Benedict and Kelley [11]. Their friction coefficient expression, which fit this data, is considered to be applicable to gear sliding loss calculations in the EHD lubrication regime where some asperity contact occurs, which is the common case.

As in [7], rolling losses were taken to be directly proportional to the EHD central film thickness following [12]. Gear tooth film thickness was calcu-

lated by the method of Hamrock [13]. In [7], film thickness was adjusted for thermal effects using Cheng's thermal reduction factor [14]. This factor causes the EHD film thickness to reach some limiting value with increasing speed. However, in the interest of simplicity, thermal effects, though potentially important at high speeds and low loads, will not be included in the simplified method to be presented.

In [7] a numerical integration method was used to compute power loss over the path of contact and was later simplified to an interval calculation. Here the method will be further simplified to a single loss expression representing the average loss across the path of contact. This is accomplished by choosing a single point along the path of contact where average sliding and rolling velocities occur to evaluate the loss expressions. In Fig. 2 a comparison of the instantaneous and average velocities as well as the instantaneous and average power losses are shown. The point at which the power loss equations are evaluated is at  $\frac{\pi}{4}$ , where the average value of sliding and rolling losses can be found from:

$$P_S = C_1 \sqrt{W V_S} \quad (1)$$

$$(P_R = C_2 \sqrt{W T_p} \sqrt{C_R}) \quad (2)$$

where the variables used in these expressions are described in the design example presented in a later section.

The simplified values of power loss, also shown in Fig. 2, approximate the area under the instantaneous loss curves to a high degree of accuracy and thus provide an accurate, simple method to determine the mesh losses. The simplified expression was found to be within 0.1 percentage points of the numerically integrated solution of [7] for the range of variables presented later in this work. The only exception to this is at extremely light loads (K-factor of 10) and high speed (greater than 40 m/sec) where under certain conditions the error can rise to 1 percentage point. This is due to the omission of a thermal correction factor to limit EHD film thickness, hence rolling power loss, at high speeds. If such operating conditions are of interest then it is suggested that a thermal EHD reduction factor such as that used in [7] be incorporated into the analysis. In addition to the mesh losses, an expression for gear windage loss was also developed in [7] from experimental data on turbine disc windage losses. To account for the oily atmosphere within the gearbox the density and viscosity of the gearbox atmosphere were corrected to reflect a 34.25 part air to 1 part oil combination as in [15]. Constant values for air density and viscosity at 339 K (150° F) and oil specific gravity of 0.9 were assumed. The expressions for pinion and gear windage were found to be:

$$P_{W,p} = C_3 \left( 1 + 2.3 \frac{\phi}{R_p} \right) n_p^{2.8} R_p^{4.6} (0.028 \mu + C_4)^{0.2} \quad (3)$$

$$P_{W,g} = C_3 \left( 1 + 2.3 \frac{\phi}{R_g} \right) \left( \frac{n_p}{m_g} \right)^{2.8} R_g^{4.6} (0.028 \mu + C_4)^{0.2} \quad (4)$$

Support bearing loss from the approximate method of Harris [10] was also included in [7]. A straddle mounted deep groove ball bearing arrangement was assumed for comparison purposes. The deep groove ball bearing losses are a function of the bearing pitch diameter, static capacity, lubricant viscosity, shaft speed and bearing load. These equations are:

$$P_{BRG} = C_5 (M_p n_p + M_g n_g) \quad (5)$$

M is a torque loss consisting of a load-dependent ( $M_L$ ) and a viscous term ( $M_V$ ). For a deep groove ball bearing:

$$M_L = 0.0009 \frac{F_{ST}^{1.55}}{C_S^{0.55}} D_m \quad (6)$$

$$M_V = \begin{cases} C_6 f_0 (vn)^{2/3} D_m^3 & \text{for } (vn) > 2000 \\ C_7 f_0 D_m^3 & \text{for } (vn) \leq 2000 \end{cases} \quad (7)$$

#### Design Example

The following is a step-by-step example of a power loss calculation using the simplified method developed in this investigation. The given geometry and operating conditions are for the example shown in Fig. 2.

Gear data:  $N_p$ , 48;  $N_g$ , 80;  $\phi$ , 8;  $\theta$ , 20°;  $m_g$ , 1.666;  $\phi$ , 0.0397 m (1.5625 in.); operating conditions:  $n_p$ , 2000 rpm;  $T_p$ , 271 N-m (2400 in.-lb);  $\mu_0$ , 0.05 N sec/m<sup>2</sup> (7.25x10<sup>-6</sup> lbf sec/in<sup>2</sup>);  $\nu_g$ , 0.60 cm<sup>2</sup>/sec (6.459x10<sup>-4</sup> ft<sup>2</sup>/sec);  $f_0$ , 2; bearing data: (medium series, 44.5 mm (1.75 in.) bore diameter, deep groove ball bearing)  $D_m$ , 0.07 m (2.75 in.);  $C_S$ , 17 436 N (3920 lbf);  $F_{ST} = W/2$ .

Length of path of contact,

$$\begin{aligned} \pi_T = C_8 \left\{ \left[ (D_p + 2/\phi)^2 - (D_p \cos \theta)^2 \right]^{1/2} \right. \\ \left. + \left[ (D_g + 2/\phi)^2 - (D_g \cos \theta)^2 \right]^{1/2} \right. \\ \left. - (D_p + D_g) \sin \theta \right\} = 0.0168 \text{ m (0.6593 in.)} \quad (8) \end{aligned}$$

Average sliding velocity,

$$\begin{aligned} V_S = 0.0262 n_p \left( \frac{1 + m_g}{m_g} \right) \pi_T \\ = 1.408 \text{ m/sec (55.27 in/sec)} \quad (9) \end{aligned}$$

Average rolling velocity,

$$\bar{V}_T = 0.1047 n_p \left[ D_p \sin \theta - \frac{\lambda_T}{4} \left( \frac{m_g - 1}{m_g} \right) \right]$$

$$= 10.56 \text{ m/sec (415.9 in/sec)} \quad (10)$$

Average normal load,

$$\bar{W} = T_p / (D_p \cos \theta) = 1892 \text{ N (425.7 lbf)} \quad (11)$$

Friction coefficient,

$$f = 0.0127 \log \left[ C_9 \bar{W} / (\mu_0 \bar{V}_S \bar{V}_T^2) \right] = 0.0287 \quad (12)$$

Average sliding power loss,

$$P_S = C_1 \bar{V}_S \bar{W} = 0.1529 \text{ kW (0.2046 hp)} \quad (1)$$

Equivalent contact radius,

$$R_{eq} = \frac{[D_p (\sin \theta) + \lambda_T / 2] [D_g (\sin \theta) - \lambda_T / 2]}{2(D_p + D_g) \sin \theta}$$

$$= 0.0171 \text{ m (0.6726 in.)} \quad (13)$$

Central EHD film thickness,

$$\bar{h} = C_{10} (\bar{V}_T \mu_0)^{0.67} \bar{W}^{-0.067} R_{eq}^{0.464}$$

$$= 1.249 \times 10^{-6} \text{ m (4.927} \times 10^{-5} \text{ in.)} \quad (14)$$

Contact ratio,

$$CR = C_{11} \lambda_T / (\bar{h} \cos \theta) = 1.787 \quad (15)$$

Average rolling power loss,

$$P_R = C_2 \bar{V}_T \bar{h} \bar{W} CR = 0.0840 \text{ kW (0.1127 hp)} \quad (2)$$

Windage losses,

$$P_{W,g} = C_3 (1 + 2.3 \sqrt{R_p}) (n_p / m_g)^{2.8} R_g^{4.6} (0.028 \mu_0 + C_4)^{0.2} = 0.0164 \text{ kW (0.0220 hp)} \quad (4)$$

$$P_{W,p} = C_3 (1 + 2.3 \sqrt{R_p}) n_p^{2.8} R_p^{4.6} (0.028 \mu_0 + C_4)^{0.2} = 0.0084 \text{ kW (0.0112 hp)} \quad (3)$$

Load dependent bearing torque loss,

$$M_{L,g} = 0.0009 F_{ST}^{1.55} C_s^{-0.55} D_m$$

$$= 0.0351 \text{ N-m (0.3107 in-lbf)} \quad (16)$$

$$M_{L,p} = 0.0009 F_{ST}^{1.55} C_s^{-0.55} D_m$$

$$= 0.0351 \text{ N-m (0.3107 in-lbf)} \quad (17)$$

Viscous bearing torque loss,

$$M_{V,g} = C_6 1.42 \times 10^{-5} f_o (v_B n_g)^{2/3} D_m^3$$

$$= 0.1079 \text{ N-m (1.024 in-lbf)} \quad (18)$$

$$M_{V,p} = C_6 1.42 \times 10^{-5} f_o (v_B n_p)^{2/3} D_m^3$$

$$= 0.1634 \text{ N-m (1.437 in-lbf)} \quad (19)$$

Total bearing torque loss,

$$M_g = M_{L,g} + M_{V,g} = 0.1430 \text{ N-m (1.335 in-lbf)} \quad (20)$$

$$M_p = M_{L,p} + M_{V,p} = 0.1985 \text{ N-m (1.748 in-lbf)} \quad (21)$$

Total bearing power loss,

$$P_{BRG} = 2C_5 (M_g n_g + M_p n_p) = 0.1194 \text{ kW (0.1601 hp)} \quad (5)$$

Total system power loss,

$$P_{TOT} = P_S + P_R + P_{W,g} + P_{W,p} + P_{BRG}$$

$$= 0.3811 \text{ kW (0.5106 hp)} \quad (22)$$

Input power,

$$P_{IN} = T_p n_p = 56.79 \text{ kW (76.16 hp)} \quad (23)$$

Gear system efficiency,



$$\eta = (P_{IN} - P_{TOT})/P_{IN} \times 100 = 99.34\% \quad (24)$$

### Comparison with Test Data

Figure 3 shows the comparison of this power loss method with the data of [16] which was generated on a back-to-back test stand with a spur gearset. In [16] speed, torque, oil flow rate, oil jet location, gear width and lubricant viscosity were test variables. The theory of [7] generally shows good agreement with the data, especially for the higher flow rate. The test data of [16] indicates that out of mesh lubrication, that is the oil jet is directed into the outlet of the gear mesh, can reduce the power loss by several hundredths of a kW. The present theory has no terms to account for this reduction.

Included in Fig. 3 for comparison is the theoretical prediction of [6]. The somewhat higher predicted loss from this theory is thought to be primarily due to the choice of friction coefficient expression which tends to overestimate the actual coefficient of friction.

### DISCUSSION OF RESULTS

The theory of [7] was used to determine the effects of various gear geometry and operating conditions on gearset efficiency. The results are shown in Figs. 4 to 10. Gearset efficiencies shown in these figures do not include the effects of bearing loss.

#### Effect of Gear Load

The effect of torque on gearset efficiency is shown in Fig. 4 for gears of three pitch diameters. The general trends shown here are typical for the wide range of gear geometries and operating conditions that were considered. At very low torque values efficiency is low due to the tare losses but efficiency rises rapidly with small increases in torque. At higher torque levels gear efficiency is relatively insensitive to torque, being generally greater than 98 percent at torque values which exceed 5 percent of the torque occurring at maximum efficiency.

The effect of pitch diameter at low torque levels is significant. Here a smaller gear is much more efficient than a large gear. At higher torque levels the differences are much less.

In Fig. 5 this data is replotted against a gear capacity factor,  $K$ , described in [17]:

$$K = \frac{C_{12} w (m_g + 1)}{D_p^3 m_g} \quad (25)$$

where

$$C_{12} = 1.45 \times 10^{-4} \text{ (SI units)} \quad C_{12} = 1.0 \text{ (English units)}$$

The allowable  $K$ -factors for helical and spur gears, tabularized in [17], generally range from a value of about 100 for low hardness-generated steel-gears to about 1000 for aircraft quality, case hardened and ground, high-speed gearing. A nominal  $K$ -rating for a general-purpose industrial drive, with 300 BHN steel gears, carrying a uniform load at a pitch-line-velocity of 15 m/sec (3000 fpm) or less would typically range from 275 to 375. The  $K$ -factor tends to normalize the efficiency data of Fig. 4. Like Fig. 4, Fig. 5 shows that larger gears generally have superior peak efficiency. However, where Fig. 4 showed that at equal, low torque levels smaller gears are more effi-

cient, in Fig. 5 the reverse is true at equal, low  $K$ -factors. This is because at equal  $K$ -factors the large gearset is operating at a significantly higher torque level (where the efficiency is greatly improved) than the smaller gearset.

Also, pitch-line-velocity is used here instead of rotational speed for its normalizing effect. Pitch-line-velocity reduces rotational speed for larger diameter gears so that a more realistic comparison can be made among different sized gearsets.

#### Effect of Diametral Pitch, Pinion Pitch Diameter, Pitch-Line-Velocity and Ratio

The "carpet" plots in Figs. 6 to 9 show the simultaneous effects of three variables; diametral pitch, pitch diameter and pitch-line-velocity, on gearset efficiency (excluding support bearing losses). These variables and gear load were found to have a greater effect on efficiency than ratio or face width. Two loading situations were chosen; (a) light load,  $K = 10$  and (b) moderate to heavy load,  $K = 300$ , close to the maximum efficiency of the gearset as shown in Fig. 4. The magnitude and trends of efficiency results at  $K = 1000$  are quite similar to those at  $K = 300$  and are not shown here.

In Fig. 6, the  $K$ -factor is constant at 300 and the ratio equals one. In this and succeeding carpet plots, the three key variables are represented along orthogonal, intersecting planes. Three values for each of the three variables are presented. The efficiency at any combination of these values occurs at an intersection point. Thus, efficiency at intermediate values can readily be found by interpolation between planes as shown in the appendix. The three values of pitch-line-velocity shown in Fig. 6, along shaded planes, are 1.3, 5.1 and 20.3 m/sec (250, 1000 and 4000 ft/min). Pitch diameter varies along one set of planes from 1.6 to 6.3 cm (4 to 6 in.) and diametral pitch varies from 4 to 16 along the other.

The most efficient combination of pinion pitch diameter and diametral pitch is the largest diameter gear having the finest-pitched teeth. Conversely the least efficient gearset is the smallest diameter gear having the coarsest pitch. At this  $K$ -factor value, an increase in pitch-line-velocity tends to increase efficiency, particularly for small, coarse-pitched gears. Although not shown, efficiency continues to increase at speeds to 40.6 m/sec (8000 ft/min) but at a much slower rate. The maximum increase in efficiency was 0.21 percentage points at a pinion diameter of 1.6 cm (4 in.) and diametral pitch of four.

Diametral pitch had the greatest effect on efficiency for any speed and gear size. At a constant diametral pitch value of 16, changes in pitch diameter and pitch-line-velocity had little effect. However, at a diametral pitch of 4, both these parameters had large effects. The higher efficiencies found with the fine pitched gears are primarily due to lower sliding velocities and, therefore, reduced power losses.

As shown in Figs. 4 and 5, large diameter gears tend to have superior performance. At a constant pitch-line-velocity the rotational speed decreases as the diameter increases. This causes a reduction in the sliding velocity which in turn limits the sliding power loss. Thus the increase in efficiency shown as diameter increases is due to a reduction in magnitude of sliding velocity.

Also shown in Figs. 4 and 5 is that an increase in pitch-line-velocity results in an increase in efficiency. As pitch-line-velocity is increased both the sliding and rolling velocities increase. In Eq. (12) it can be seen that an increase in either of these

velocities will reduce the coefficient of friction. This reduction in friction coefficient tends to reduce the sliding power loss so that the sliding loss does not increase directly with pitch-line-velocity as does the input power. The net result is that the efficiency is improved.

In Fig. 7 the results of changing gear reduction ratio from one to six at  $K = 300$  are shown. Since pinion diameter is held constant a change in ratio means a change in gear diameter. A comparison of Figs. 6 and 7 reveals that ratio has a negligible effect on efficiency at a pitch-line-velocity of 20.3 m/sec (4000 ft/min) and a small effect at lower pitch-line-velocities. At low speeds the efficiency of small, coarse-pitched gears are most improved by an increase in ratio. A maximum increase in efficiency was found to be approximately 0.5 percentage points for a change in ratio of one to six. The reason for lower losses at the higher ratios is due to a slight reduction in sliding velocities. However, overall the effect of ratio on efficiency was judged to be slight.

In Fig. 8 the K-factor has been reduced to 10 and ratio is still equal to one. This is essentially an unloaded gearset and the losses are almost entirely the tare losses - the rolling and windage losses. Gear tooth sliding losses are insignificant since the tooth loading is very low. The effect of the variables at  $K = 10$  are significantly different than at  $K = 300$ . The effect of pitch-line-velocity is reversed. The most efficient pitch-line-velocity is the lowest value and a significant reduction in efficiency occurs as pitch-line-velocity increases. This is due to the fact that the tare losses are a strong function of rotational speed. The efficiencies are much lower since the power being transmitted is very low.

The effect of increased efficiency with increased diameter remains the same here at the lightly loaded case. The effect of diametral pitch on efficiency is greatly reduced at this low K-factor. Only at the lowest pitch-line-velocity, where sliding losses are still significant, 1.3 m/sec (250 ft/min), will the efficiency still increase appreciably with finer pitched gear teeth. At higher pitch-line-velocities where the sliding loss becomes insignificant relative to the rolling loss, the diametral pitch has virtually no effect on efficiency. Efficiency data calculated at 5.1 m/sec (1000 ft/min) were intentionally omitted in Fig. 8 for clarity since these data were within 0.5 percentage points of the data at 1.3 m/sec (250 ft/min).

In Fig. 9 the gear ratio was increased to six at  $K = 10$ . As mentioned previously, this is equivalent to increasing the gear diameter by a factor of six. At 1.3 m/sec (250 ft/min) ratio has little effect on efficiency. However, at 20.3 m/sec (4000 ft/min) the increased ratio causes an approximate 0.5 percentage point drop in efficiency while at 40.6 m/sec (8000 ft/min) efficiency is substantially reduced by about 4 percentage points. Thus ratio has its strongest effect at high pitch-line-velocity and light loads where rolling and windage losses are the main source of power loss.

#### Effect of Face Width/Diameter Ratio

In the previous carpet plots, the  $\mathcal{F}/D$  ratio was held constant at 0.5. In Fig. 10 the effect of  $\mathcal{F}/D$  ratio on efficiency at several values of pitch-line-velocity and K-factors is shown. In most cases the efficiency change is very small, less than 0.2 percentage points, for a range of  $\mathcal{F}/D$  ratios of 0.5 to 2.0. However, at pitch-line-velocities above 20.3 m/sec (4000 ft/min) at a low K-factor of 10, the var-

iation in efficiency with  $\mathcal{F}/D$  ratio is somewhat more significant primarily due to the effects of windage. The maximum variation occurs at 40.6 m/sec (8000 ft/min) where the narrowest gearset ( $\mathcal{F}/D = 0.5$ ) is less efficient than the widest gearset by 4.1 percentage points. However, for a wide range of operating conditions the  $\mathcal{F}/D$  ratio does not significantly affect efficiency.

#### Breakdown of Gear System Loss

A theoretical breakdown of the various components of gear system power loss for the test gears of [16] is shown in Fig. 11. At low pinion speeds (Fig. 11(a)), the sliding loss accounts for most of the system losses. However, at higher speeds (Figs. 11(b) and (c)), the pinion bearing losses become increasingly more important. At a pinion speed of 2000 rpm, the gear and pinion windage losses, which are often neglected, contribute as much as 10 percent of the total power loss and should not be ignored.

At low torque levels, the sliding loss is low since this loss is a direct function of load. The rolling loss is relatively insensitive to torque, being proportional to film thickness, so it is a major source of power loss at low torques, particularly at the higher speeds.

Figure 11(c) clearly illustrates the potential pitfall of disregarding the speed dependent losses when computing gearbox losses, which is all too often the case. Even at the full load value of 271 N-m (200 ft/lbf) where the sliding losses are a maximum, they still represent about one-half of the total gear mesh losses which excludes bearing losses. It is also instructive to note that at this operating condition, the total support bearing losses are nearly 80 percent as large as the gear sliding losses. Good estimates of gear rolling and windage losses along with support bearing losses are vital to accurately determining the power consumption of the gearbox.

Finally, Fig. 11 illustrates that the unloaded or tare losses associated with a gearset can be a surprisingly high percentage of the loaded power losses. Of course methods which use just a sliding coefficient of friction to predict losses will completely miss this tare loss since without load there can be no sliding power loss. This is why these methods significantly overestimate part-load efficiency.

In Fig. 12 this tare or unloaded power loss is plotted as a percentage of full load loss over a wide range of pitch-line-velocities and gear sizes for the gearset studied in Figs. 4 and 5. This tare loss is comprised entirely of rolling, windage and support bearing power loss. The support bearings were scaled in proportion to the gear size as shown.

From Fig. 12, it is apparent that pitch-line-velocity has a more dominant effect than diameter on percentage tare loss, since at equal pitch-line-velocity the large gearset is actually turning slower. Over the range of operating conditions considered, tare losses are appreciable and should not be overlooked when determining required cooling capacity or idling power consumption.

#### SUMMARY

A method to calculate gear mesh power losses from the conditions occurring at one point along the path of contact was developed. The sliding and rolling velocities occurring at this point can be used to compute the average sliding and rolling-traction power losses for the mesh. In addition, expressions are given to determine gear windage and support bearing

losses. This approximate method was compared to the more exact numerical method of [7]. A design example was given to illustrate the application of the method developed. The analysis presented was used to generate efficiency plots at low and moderate to high loads which showed which gear geometries and operating variables lead to the highest gearset efficiencies. The following results were obtained from this investigation:

1. The single point, approximate gear loss method gave efficiency results within 0.1 percentage points of the full numerical integration solution of [7]. The only exception occurs at light load and high speeds (40 m/sec) where the lack of a thermal correction factor to limit EHD film thickness causes the deviation to increase to 1 percentage point.

2. Under moderately-to-heavily loaded conditions (K-factor = 300), an increase in diametral pitch, pitch diameter and pitch-line-velocity causes an increase in gearset efficiency. However, under light loads (K-factor = 10), an increase in pitch-line-velocity causes an efficiency loss and an increase in diametral pitch has only a slight benefit on gear efficiency primarily at low velocities.

3. Gear ratio and face width-to-diameter ratio generally had minor effects on efficiency except at light loads where high ratio and narrow gearsets tend to be less efficient, particularly at high pitch-line-velocities (above 20 m/sec).

4. Rolling-traction power losses, support bearing power loss and windage losses, to a lesser extent, were significant portions of the total gear system loss. Unloaded or tare gear power losses at operating speed can be as much as 65 percent of the loaded, maximum power loss.

#### APPENDIX

To determine the efficiency of a gearset not located along the axes appearing on a carpet plot, a three dimensional interpolation must be done. Since the value of the three independent variables are uniformly spaced along the carpet plot axes a linear interpolation is all that is required. An example of such an interpolation is shown in Fig. 13 where Fig. 9 is interpolated for a pinion diameter of 2.8 cm (7 in.), diametral pitch of 10 and a pitch-line-velocity of 30 m/sec (6000 ft/min). First, planes of constant pinion diameter, diametral pitch and pitch-line-velocity equal to the required values are established by linear interpolation along the boundaries where values are given. As these planes are established, intersection lines between planes will form leading to one intersection point. This point establishes the required gearset efficiency by projection to the efficiency scale. In this case, the required gearset efficiency is determined to be 94.3 percent.

#### REFERENCES

1. Anderson, N. E., and Loewenthal, S. H., "Effect of Geometry and Operating Conditions on Spur Gear System Power Loss," ASME paper no. 82-G2/DET-39; Sept. 1980.
2. Shipley, Eugene E., "Loaded Gears in Action," Gear Handbook, 1st. ed., D. W. Dudley, ed., McGraw-Hill, New York, 1962, ch. 14, pp. 14-1 - 14-60.
3. Buckingham, Earle, "Efficiencies of Gears," Analytical Mechanics of Gears, Dover, New York, 1963, ch. 19, pp. 395-425.
4. Merritt, H. E., "Efficiency and Testing," Gear Engineering, Wiley, New York, 1972, ch. 22, pp. 345-357.
5. Martin, K. F., "A Review of Friction Predictions in Gear Teeth," Wear, Vol. 49, No. 2, Aug. 1978, pp. 201-238.
6. Chiu, Y. P., "Approximate Calculation of Power Loss in Involute Gears," ASME Paper 75-PTG-2, Oct. 1975.
7. Anderson, N. E. and Loewenthal, S. H., "Spur-Gear-System Efficiency at Part and Full Load," NASA TP-1622, AVRAOCOM TR 79-46, 1980.
8. Mann, R. W., and Marston, C. H., "Friction Drag on Bladed Discs in Housings," Journal of Basic Engineering, Vol. 83, No. 4, Dec. 1961, pp. 719-723.
9. Daily, J. W., and Nece, R. E., "Chamber Dimension Effects on Induced Flow and Frictional Resistance of Enclosed Rotating Disks," Journal of Basic Engineering, Vol. 82, No. 1, Mar. 1960, pp. 217-232.
10. Harris, T. A., Rolling Bearing Analysis, Wiley, New York, 1966.
11. Benedict, G. H. and Kelley, B. W., "Instantaneous Coefficients of Gear Tooth Friction," ASLE Transactions, Vol. 4, No. 1, Apr. 1961, pp. 59-70.
12. Crook, A. W., "The Lubrication of Rollers. IV. Measurements of Friction and Effective Viscosity," Philosophical Transactions of the Royal Society (London), ser. A, Vol. 255, No. 1056, Jan. 17, 1963, pp. 281-312.
13. Hamrock, B. J. and Dowson, D.: "Isothermal Elastohydrodynamic Lubrication of Point Contacts. III - Fully Flooded Results," Journal of Lubrication Technology, Vol. 99, No. 2, Apr. 1977, pp. 264-276.
14. Cheng, H. S., "Prediction of Film Thickness and Sliding Frictional Coefficient in Elastohydrodynamic Contacts," ASME Design Engineering Technology Conference, 1st. ASME, New York, 1974, pp. 285-293.
15. Bowen, C. W., Braddock, C. E., and Walker, R. D., "Installation of a High-Reduction-Ratio Transmission in the W1-1 Helicopter," BNR-299-099-112, Bell Helicopter Co., Fort Worth, Texas, 1969 (USARVLABS-TR-60-57, AD-855747).
16. Fletcher, H. A. G., and Bamborough, J., "Effect of Oil Viscosity and Supply Conditions on Efficiency of Spur Gearing," NEL-138, National Engineering Laboratory, Glasgow, Scotland, 1964.
17. Wellauer, E. J., "Lead Rating of Gears," Gear Handbook, McGraw-Hill, New York, 1st. ed., 1962, D. W. Dudley, ed., ch 13, pp. 13-1 - 13-48.



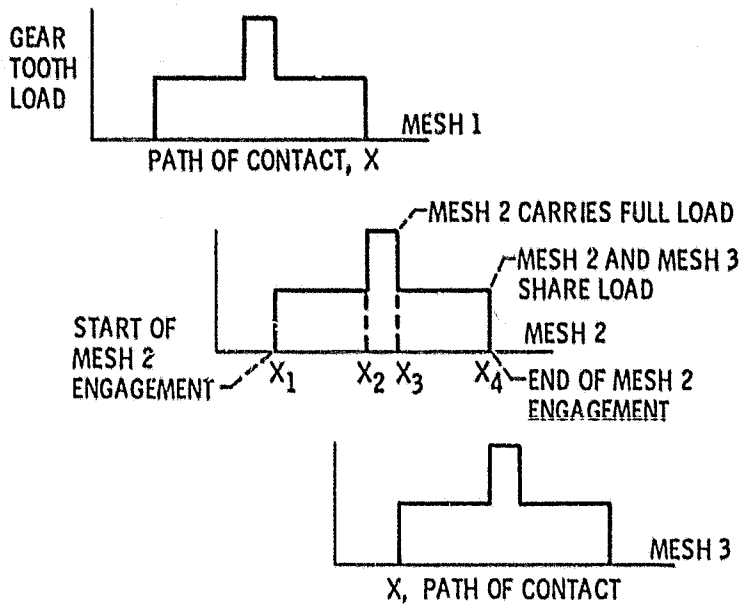


Figure 1. - Tooth load sharing diagram.

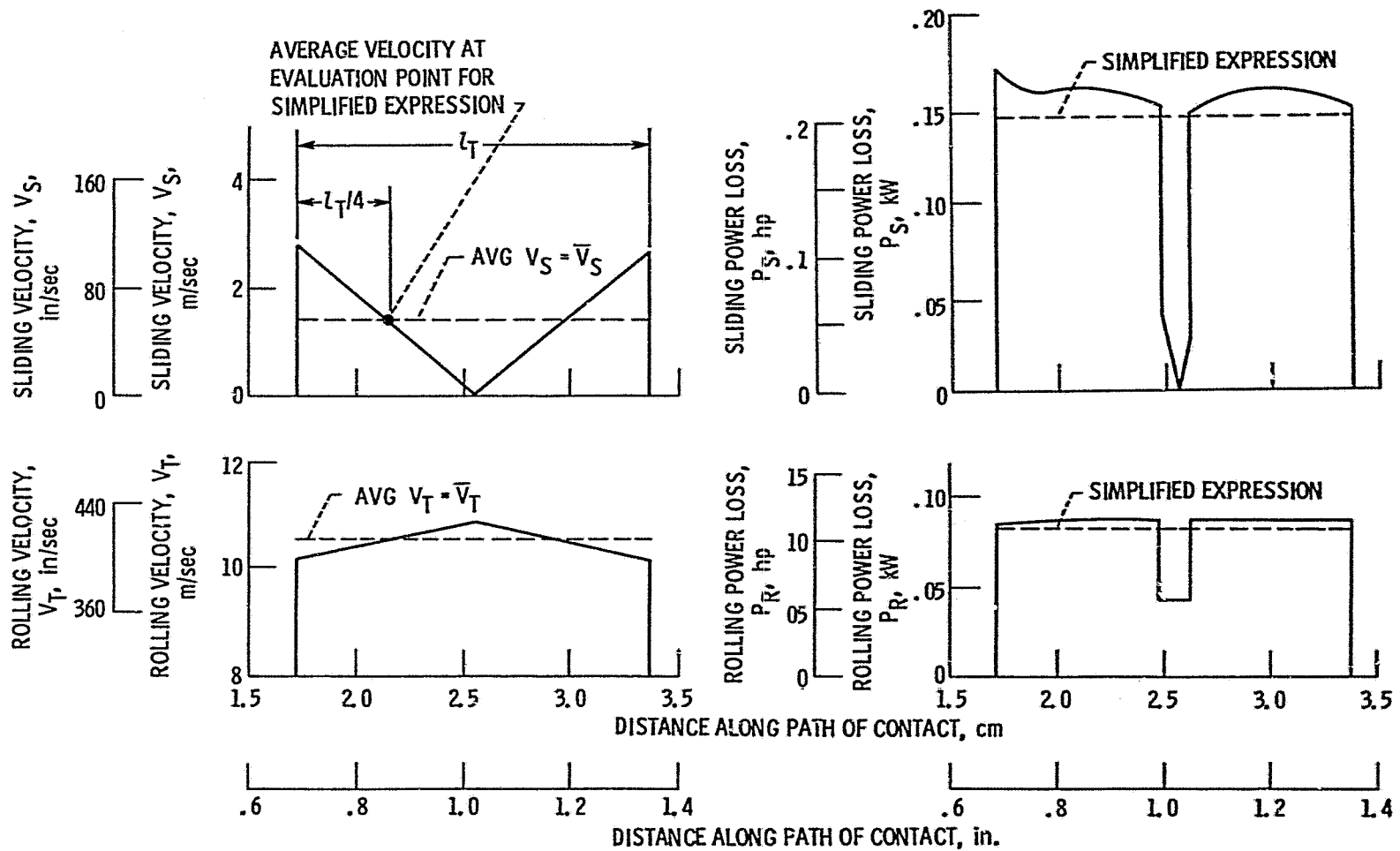


Figure 2. - Instantaneous and average values of sliding velocity, rolling velocity, sliding power loss and rolling power loss across the path of contact of test gears from [16]. Pinion speed, 2000 rpm; pinion torque, 271 N-m (200 ft-lbf); pinion pitch diameter, 15.2 cm (6 in.); ratio, 1.67; diametral pitch, 8; pressure angle,  $20^\circ$ ; pinion width/diameter ratio, 0.26; lubricant viscosity, 60 cs.

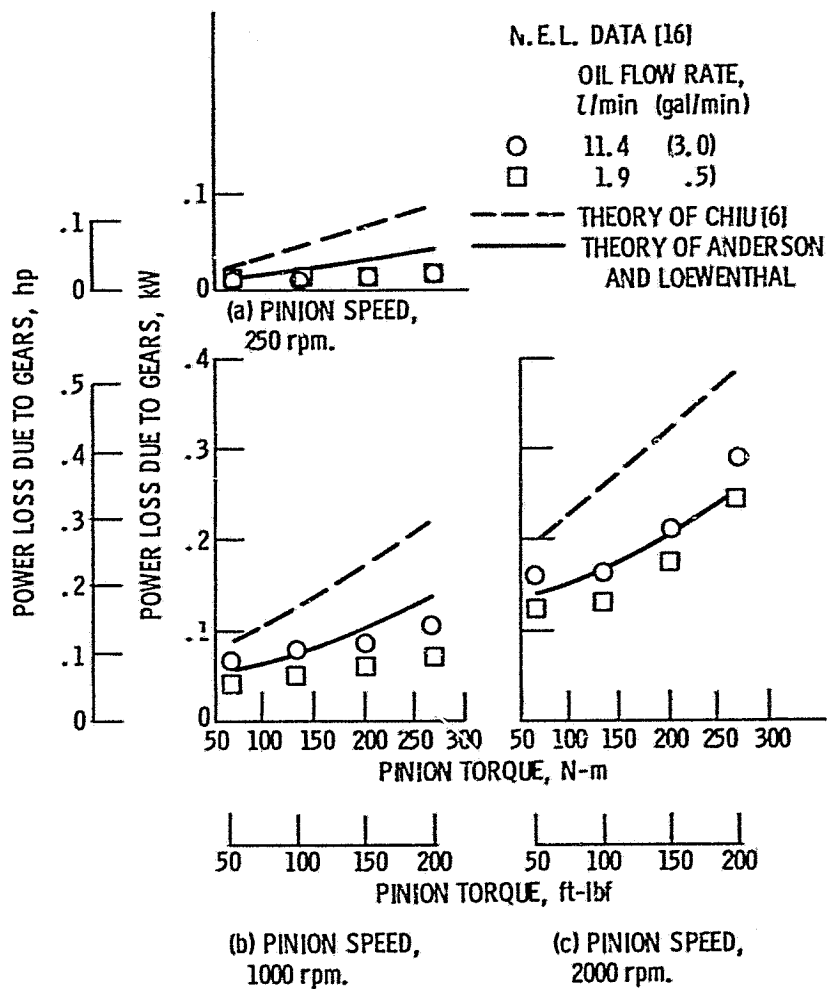


Figure 3. - Comparison of predicted gear power loss for into mesh lubrication with data of [16]. Pinion pitch diameter, 15.2 cm (6 in.); ratio, 1.67; diametral pitch, 8; pressure angle, 20°; pinion width/diameter ratio, 0.26; lubricant viscosity, 60 cs.

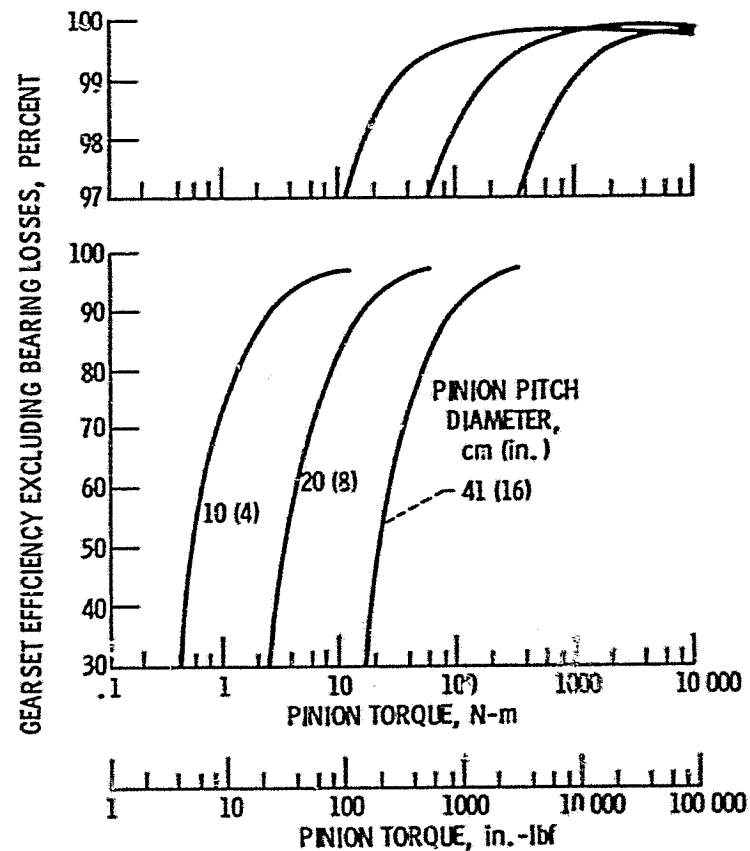


Figure 4. - Effect of torque on gasket efficiency for three pitch diameter pinions. Pitch line velocity, 20.3 m/sec (4000 ft/min); ratio, 1.0; diametral pitch, 32; pressure angle, 20°; pinion width/diameter ratio, 0.5; lubricant viscosity, 30 cp.

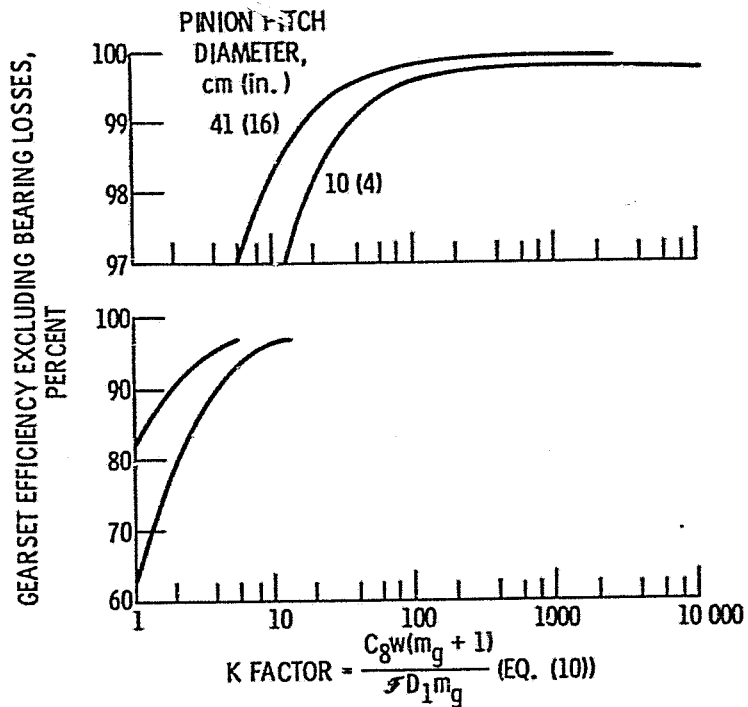


Figure 5. - Effect of pitch diameter on gearset efficiency as a function of K factor. Pitch line velocity, 20.3 m/sec (4000 ft/min); ratio, 1.0; diametral pitch, 32; pressure angle, 20°; pinion width/diameter ratio, 0.5; lubricant viscosity, 30 cp.

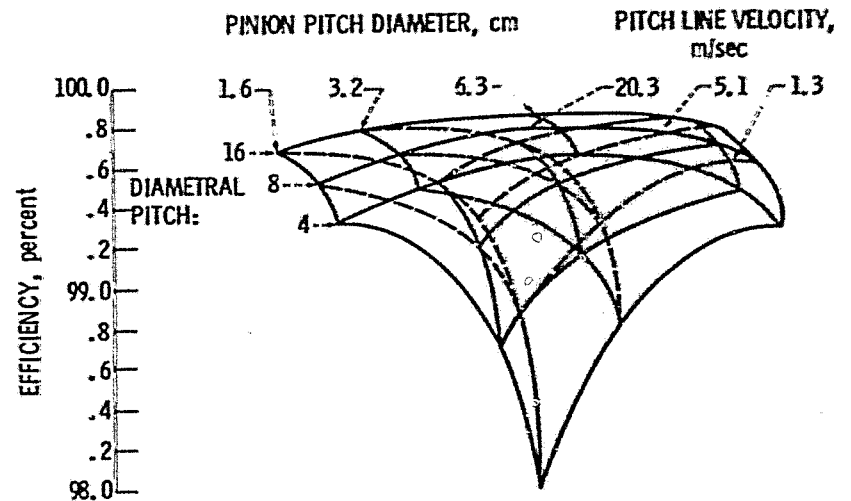


Figure 6. - Effect of pinion diameter, diametral pitch and pitch line velocity on gearset efficiency at a K-factor of 300; ratio, 1.0; pressure angle, 20°; pinion width/diameter ratio, 0.5; lubricant viscosity, 30 cp.

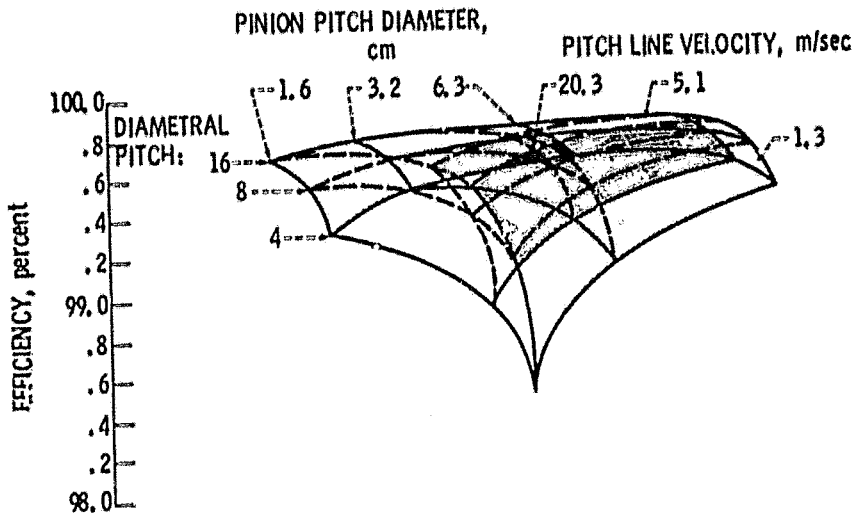


Figure 7. - Effect of pinion diameter, diametral pitch and pitch line velocity on gearset efficiency at a K-factor of 300; ratio, 6; pressure angle,  $20^\circ$ ; pinion width/diameter ratio, 0.5; lubricant viscosity, 30 cp.

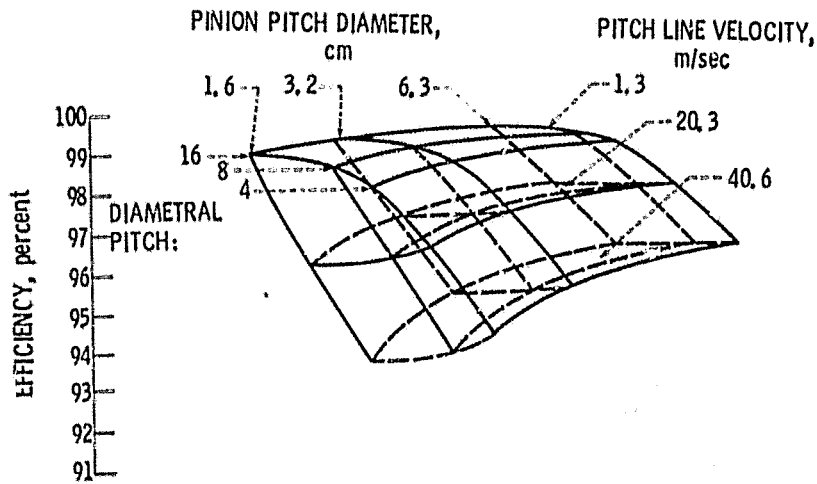


Figure 8. - Effect of pinion diameter, diametral pitch and pitch line velocity on gearset efficiency at a K-factor of 10; pressure angle,  $20^\circ$ ; pinion width/diameter ratio, 0.5; lubricant viscosity, 30 cp.

ORIGINAL PAGE IS  
OF POOR QUALITY



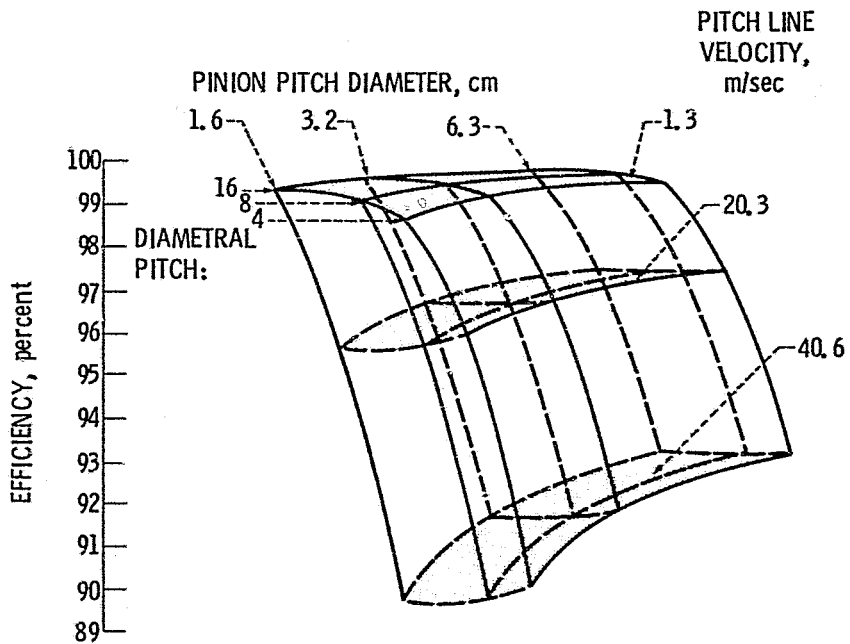


Figure 9. - Effect of pinion diameter, diametral pitch and pitch line velocity on gearset efficiency at a K-factor of 10; ratio, 6; pressure angle,  $20^\circ$ ; pinion width/diameter ratio, 0.5; lubricant viscosity, 30 cp.

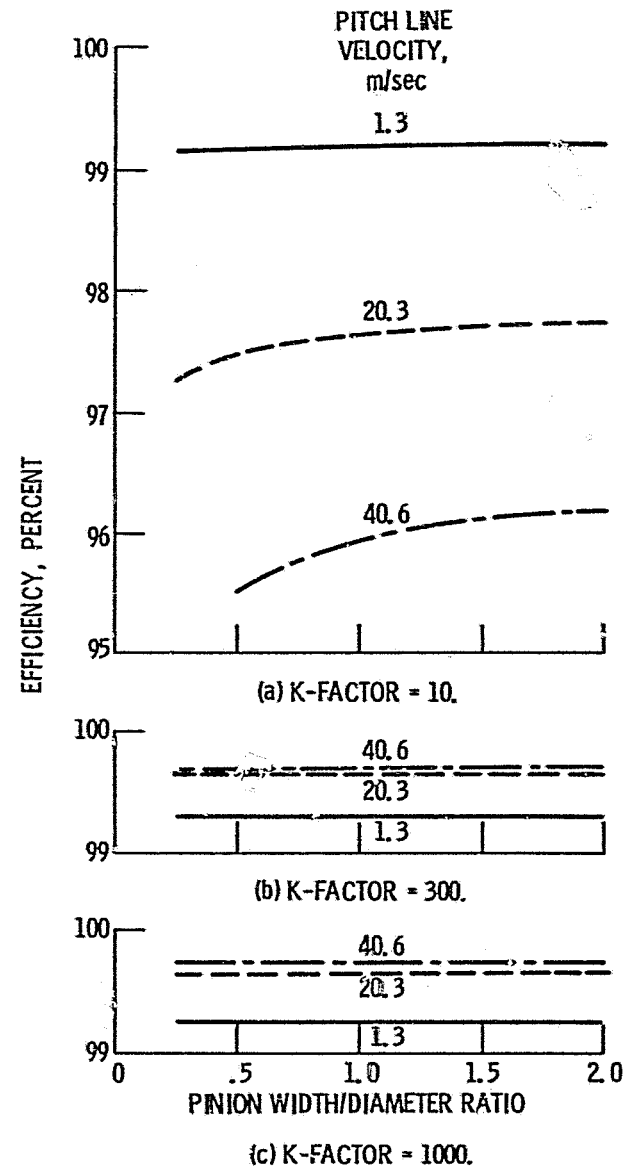


Figure 10. - Effect of pinion width/diameter ratio on gearset efficiency at various K-factors (gear loads). Pinion pitch diameter = 3.2 cm (8 in.); ratio, 1.0; diametral pitch, 8; pressure angle,  $20^\circ$ ; lubricant viscosity, 30 cp.

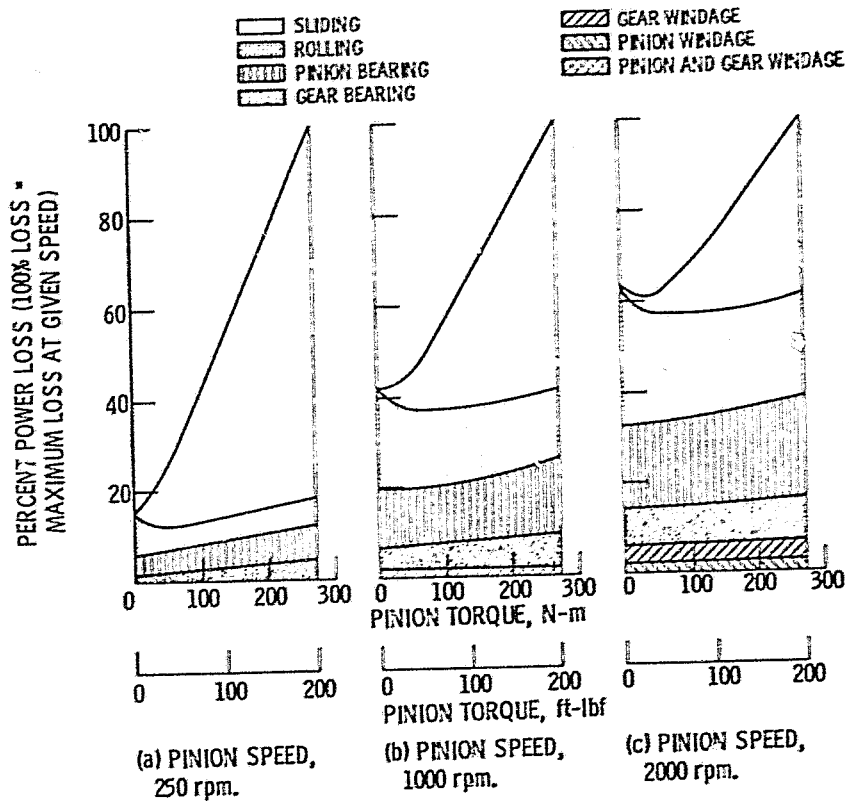


Figure 11. - Comparison of gearbox power loss components. Pinion pitch diameter, 15.2 cm (6 in.); ratio, 1.67; diametral pitch, 8; pressure angle,  $20^\circ$ ; pinion width/diameter ratio, 0.26; lubricant viscosity, 60 cs; support bearings, light series, 44.5 mm (1.75 in.) bore diameter deep-groove ball bearings. Operating conditions from figure 3.

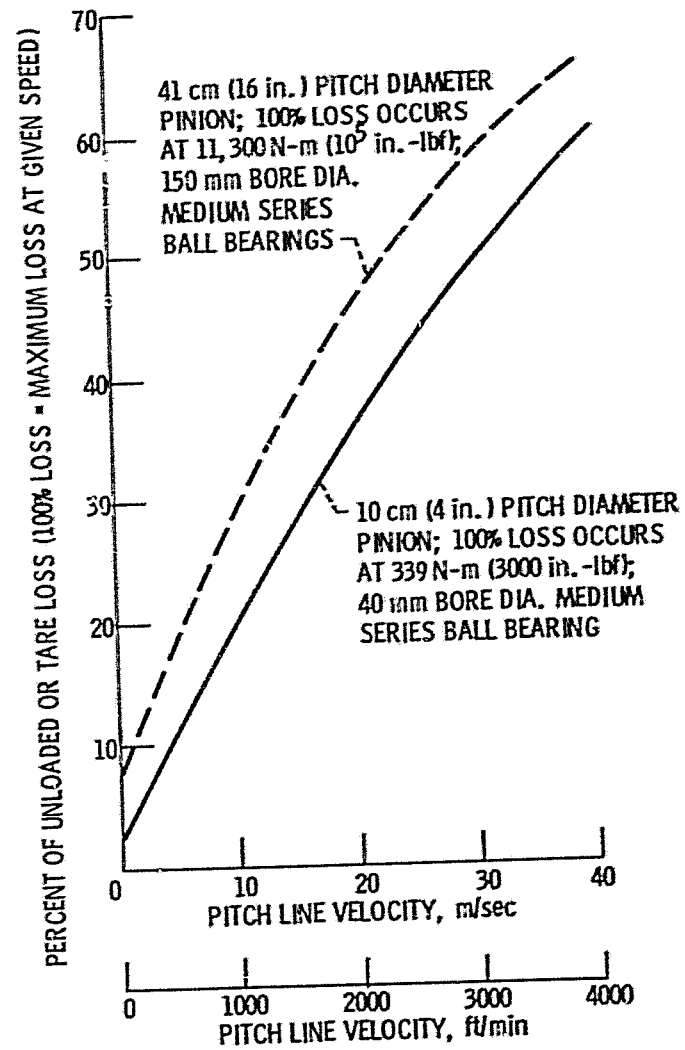


Figure 12. - Percent tare loss as a function of pitch line velocity and pitch diameter. Ratio, 1.0; diametral pitch, 8; pressure angle,  $20^\circ$ ; pinion width/diameter ratio, 0.5; lubricant viscosity, 30 cp.

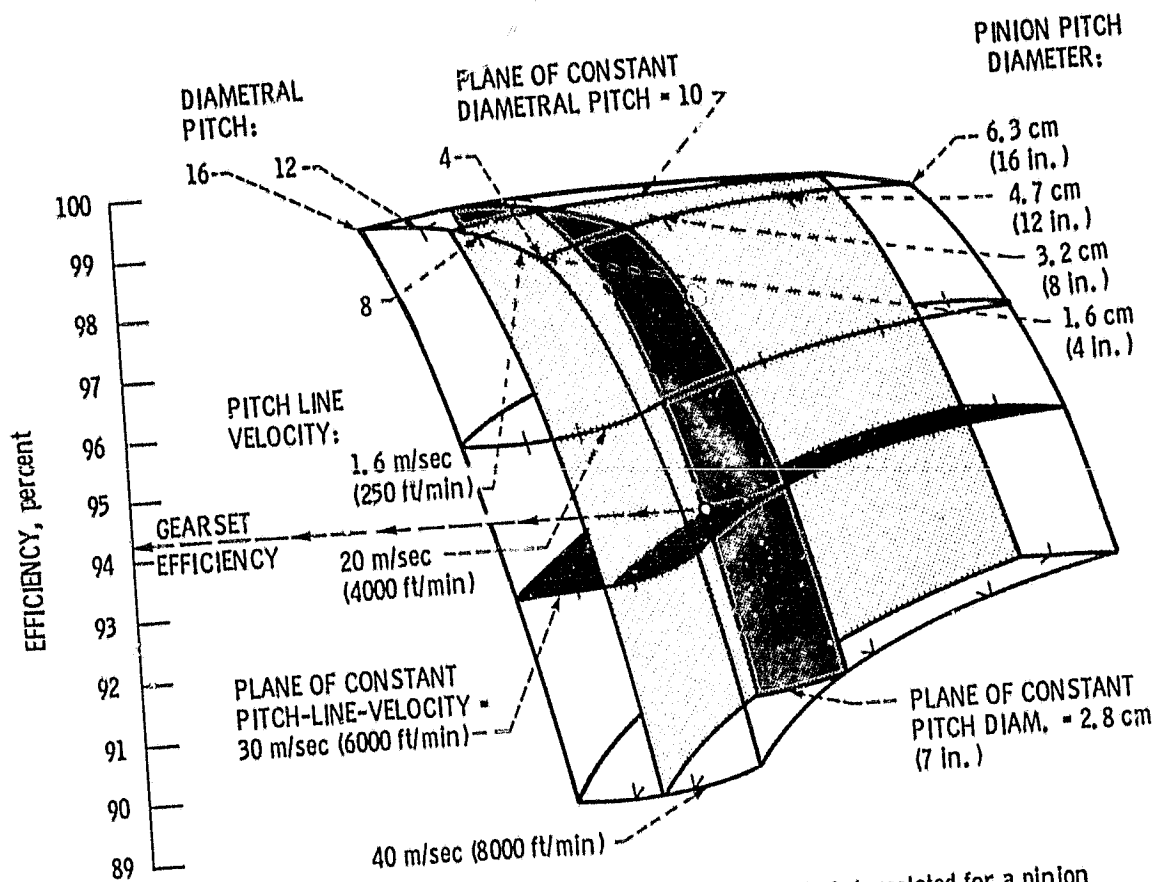


Figure 13. - Example of interpolation on a carpet plot. Figure 9 is interpolated for a pinion diameter of 2.8 cm (7 in.), diametral pitch, 10 and pitch line velocity of 30 m/sec (6000 ft/min).